Electron Heating Model in μ10 Ion Thruster

IEPC-2017-489

Presented at the 35th International Electric Propulsion Conference
Georgia Institute of Technology • Atlanta, Georgia • USA
October 8 – 12, 2017

Giulio Coral[1]
The University of Tokyo, Bunkyo-ku, Tokyo, 113-8654, Japan

Ryudo Tsukizaki[2], Kazutaka Nishiyama[3], and Hitoshi Kuninaka[4]
Japan Aerospace Exploration Agency, Sagamihara, Kanagawa, 252-5210, Japan

Abstract: Electrons in the μ10 ion thruster gain energy from a microwave input through electron cyclotron resonance. A model defining the properties of different chamber regions has been developed and verified through Langmuir probes. Power absorption efficiency has been measured with the same technique and by analyzing performance parameters. A cathodoluminescence based method to measure electron currents was demonstrated, although not applied to this case.

Nomenclature

C_i	=	ion production cost
C_0	=	primary electron utilization factor
D	=	diffusion coefficient
f_s	=	ion current ratio
I_{CL}	=	cathodoluminescence intensity
I_e	=	electron current
n_e	=	electron density
P_μ	=	microwave power
T_e	=	electron temperature
V_{ECR}	=	ECR voltage gain
α	=	microwave power absorption efficiency
Γ	=	particle flux
ε_p*	=	baseline plasma ion energy cost
η	=	propellant utilization efficiency
ω_c	=	electron cyclotron frequency

I.Introduction

Ion engines utilize power for plasma production and ion acceleration. While the second is directly related to the engine thrust, the first is substantially "lost" power, utilized purely for plasma production[4]. For this purpose, minimizing and optimizing the power absorption in the plasma source has potential to increase the thrust per unit power.

Although performance has been improved over time[6,8-10], main limitation of μ10 compared to same-class DC and RF competing thrusters are the inefficiencies in the plasma production process. A theoretical model describing how

[1] PhD Candidate, Grad. School of Engineering – Dept. of Aeronautics and Astronautics, giuliocoral@ep.isas.jaxa.jp
[2] Assistant Professor, Institute of Space and Astronautical Science, ryudo@ep.isas.jaxa.jp
[3] Associate Professor, Institute of Space and Astronautical Science, nishiyama@ep.isas.jaxa.jp
[4] Vice-President, Institute of Space and Astronautical Science, kuninaka@isas.jaxa.jp

power is transferred to plasma in the chamber and to the ion beam has been developed in the past in this laboratory specifically for ECR ion sources[11], based on the equivalent for DC ion sources[1]. It was pointed out how further investigation of the microwave power absorption efficiency α and the related plasma phenomena would be needed to improve our understanding of the ion thruster, and potentially allow further improvements.

II.Electron Heating Model

A. Active-Passive-Loss Regions Model

Consider two magnets with opposite orientation in a closed chamber with a microwave field in it. Electron cyclotron resonance (ECR) will occur over the isomagnetic surface at which $f_E = \omega_c/2\pi$. The chamber boundary and the ECR region define the limits between the three regions we will call:

- *Active* region: close magnetic mirrors crossing the ECR isomagnetic. Electrons cross it multiple times gaining eV_{ECR} energy at each passage.
- *Passive* region: close magnetic mirrors not crossing the ECR isomagnetic. No electron heating occurs, electrons are lost with their initial energy E_0.
- *Loss* region: open magnetic mirrors (limited by the chamber), crossing the ECR isomagnetic. Electrons can gain up to $2eV_{ECR}$ before getting lost to the walls.

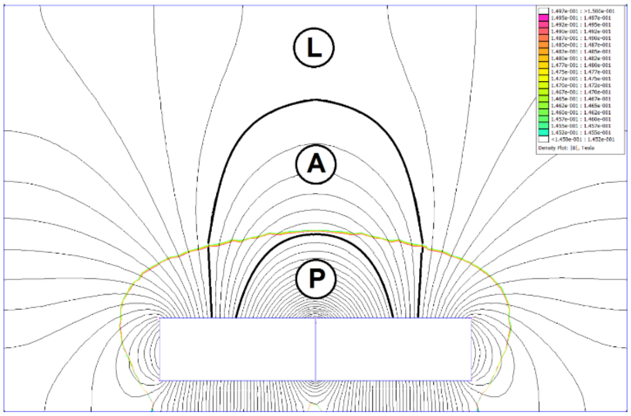

Figure 1. Active-Passive-Loss Region Model in an Arbitrary Chamber.

While this description is based on single particle dynamics, collective behavior of plasma clearly mitigates these through thermalization of the electron distribution and across-B diffusion.

Hence, although only the *active* region is capable of sustaining plasma production, a lower plasma density is present in the other two as well.

B. Diffusion across Regions

For an isothermal distribution of particles, diffusion theory defines the flux across a magnetic field as[2]:

$$\boldsymbol{\Gamma} = \mathrm{n}\,\boldsymbol{v} = -D\,\boldsymbol{\nabla} n \tag{1}$$

The assumption of isothermal plasma becomes unnecessary if we state that *no interaction with other charged particles* (definition of weakly ionized) *implies no interaction with other charged particles with a different energy*. In this case, we can introduce an arbitrary distribution of electrons $F(T_e)$ in Eq. (1), obtaining:

$$\boldsymbol{\Gamma} = \mathrm{n}\,\boldsymbol{v} = -D\,\boldsymbol{\nabla} F(T_e) \tag{2}$$

We will now demonstrate this on a Maxwell-Boltzmann distribution of electrons centered at 4eV, which is the assumption we use for the μ10 ECR ion source, truncating it at 30eV when values become negligible. As we want to observe the general case, we disregard the magnitude of n_e and D, and normalize the results to make them easily comparable. Note that the relative distribution of temperature for $\boldsymbol{\Gamma}$, once the initial $F(T_e)$ is given, is not dependent on any of these parameters.

This analysis points out is that if in the *Active* region of our ECR ion source we have a Maxwell-Boltzmann distribution peaking at a certain electron temperature, the flux $\boldsymbol{\Gamma}$ will have a different one, peaking at higher

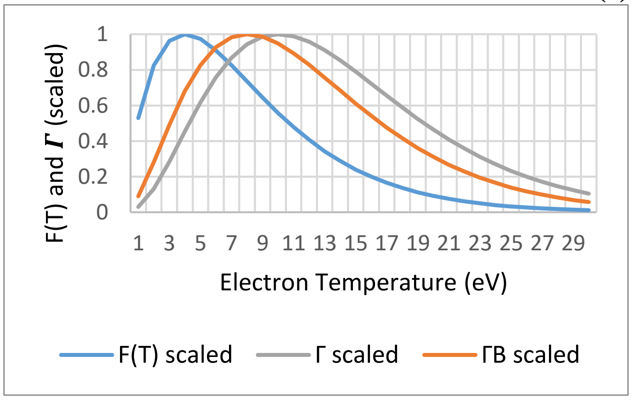

Figure 2. 4eV Maxwellian Distribution and Resultant Flux.

electron temperatures (10eV with classical diffusion, 8eV with Bohm diffusion).

C. Microwave Power Absorption

The microwave power absorption efficiency α is defined as the ratio between the power absorbed by electrons that will produce ionization and the microwave power input P_μ:

$$\alpha = 4\frac{V_{ECR} I_e}{P_\mu} \tag{3}$$

Notice that our definition includes electrons at lower temperatures, but not electrons lost to the walls. Since an electron will cross the ECR region 4 times before getting back to its initial direction and position, a factor of 4 is added.

A few more analytical steps will lead us to the alternative form[3]:

$$\alpha = \frac{2eA_{min}\pi E_{ECR}^2}{P_\mu \left|\frac{\partial B}{\partial s}\right|_{ECR}} n_e \left|-cos\theta\right|_{\theta_{min}}^{\theta_{ECR}} \tag{4}$$

Which allows to better understand the design and measured parameters that affect α. The parameters measured experimentally will be E_{ECR} and n_e.

Furthermore, α is related to the C_i as:

$$C_i = \frac{\varepsilon_P^*}{\alpha\ f_s\ (1 - e^{-C_0 \dot{m}(1-\eta)})} \tag{5}$$

Which allows us, for different values of η, to plot the hypothesized correlation between them as shown in Fig. 3.

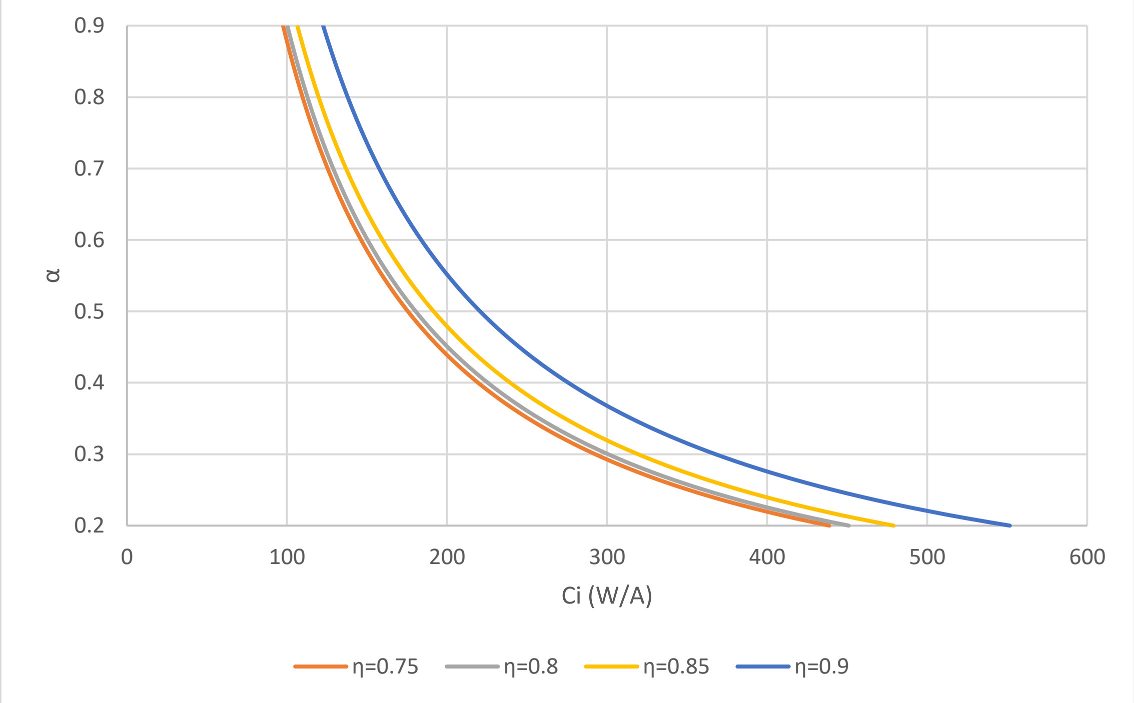

Figure 3. Estimate of α as Function of C_i.

Based on the previous considerations on the different regions, it’s clear how α will be meaningfully defined only in the *active* region.

III.Langmuir Probe Experiments

A. Verifying the Active-Passive-Loss Region Model

The experiment proposed to verify the validity of the *active-passive-loss* model consists in three planar Langmuir probes placed in correspondence of the regions, close to the surface of the magnets to reduce the disturbance produced.

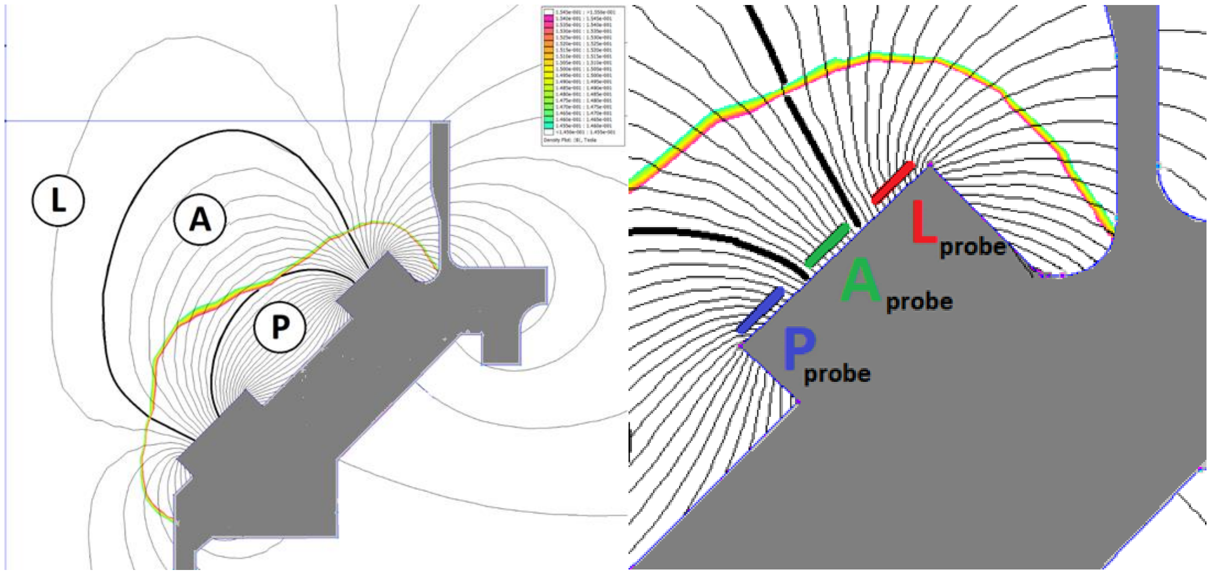

Figure 4. Active-Passive-Loss Region Model Applied to the µ10 Chamber and Probe Location

Langmuir probe are 2mm wide and 10mm long, with negligible thickness. They are swept with a bipolar power supply in a ±80V range. µ10 was operated in the 2 grids configuration (no deceleration grid), with 2.45sccm (2DC:1WG) Xe gas and 34W input power. A sample of the output produced is shown in linear and semilogarithmic plots.

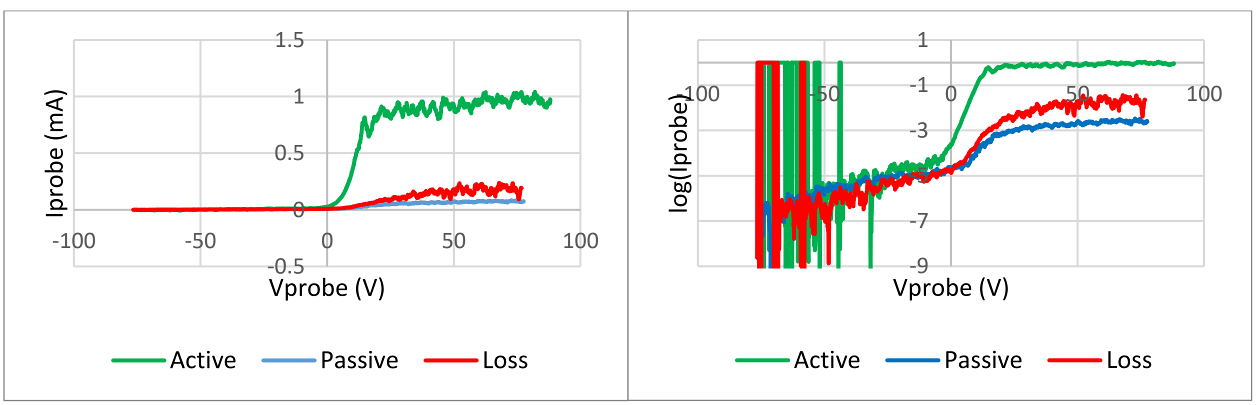

Figure 5. Linear and Semilogarithmic Langmuir Probe Curves in Active-Passive-Loss Regions

The averaging over 5 measurements per probe, we can summarize our results for n_e and T_e as in Table 1.

	n_e	T_e
Active	$3.33*10^{16}$ particles/m^3	4.01eV
Passive	$1.06*10^{15}$ particles/m^3	7.65eV
Loss	$4.42*10^{15}$ particles/m^3	7.79eV

Table 1. Electron Density and Temperature for Active-Passive-Loss Regions

These results are in good agreement the hypotheses we made. One order of magnitude higher electron density in the Active region supports the hypothesis that no ECR heating occurs in the Passive and Loss regions. The higher baseline electron temperature in these regions, on the other hand, support the non-isothermal diffusion model proposed, together with the 1:4 ratio between their densities (which further supports Bohm diffusion).

B. Measuring the Microwave Power Absorption Efficiency

As previously discussed, measurement of α is meaningful only in the *active* region. Using the previously placed central probe, we will determine how α varies with mass flow (2.1-2.85sccm) and microwave power input (28-40W). The parameter of Eq. (4) will be obtained as:

- A_{min}, θ_{ECR}, θ_{min} and $\partial B/\partial s$ are determined from a FEMM simulation of the ECR ion source
- P_μ is an input parameter
- E_{ECR} is obtained with electro-optical probe, although with limited spatial resolution[5]
- n_e is calculated from the Langmuir probe curves, and multiplied by R, calculated as an average for the magnetic mirrors in the *Active* region

During this experiment, at low mass flow (2.1sccm) transition from a low beam current mode to standard operation (with probe positively biased) was observed, making the results incomparable with the others due to the different plasma state.

Experiment results show α tends to decrease with increasing P_μ, with a substantially similar trend (excluding the low beam current mode previously described. The absolute value is close enough to the 0.5-0.6 range predicted by previous literature.

On the contrary, for a given P_μ no substantial variation in α is observed at different $\dot{m}$. The peak observed at 28W-2.4sccm doesn't seem to reflect an existing trend, with all other measurements showing α is substantially independent from $\dot{m}$.

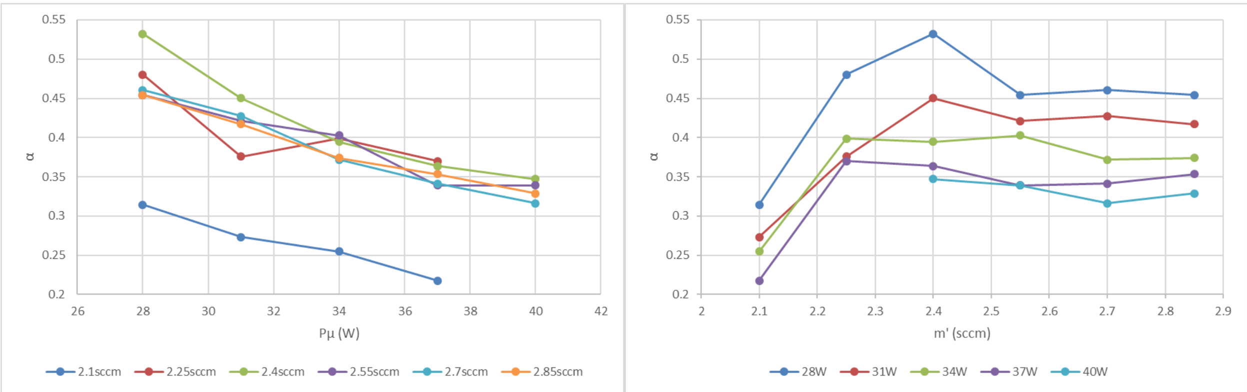

Figure 6. Microwave Power Absorption Efficiency as Function of Microwave Power and Mass Flow

IV. Alternative Measurement Techniques

The well-known disturbances produced by Langmuir probes led us to aim for less invasive techniques to measure α and other parameters.

A. Curve Fitting Approach

We previously discussed Eq. (5), relating C_i, α and η.

It's clear how, after the other parameters are determined, α could be calculated based on C_i and η, which are simply derived from I_B, P_μ and $\dot{m}$, all parameters that can be easily obtained. It's important to notice how, for low values of η, C_i tends asymptotically to:

$$C_i \to \frac{\varepsilon_P^*}{\alpha \ f_s} \tag{6}$$

In this way, the η-C_i curve can be fitted to obtain α. Previous literature assumed ε_p^* as constant, which would lead to a horizontal asymptote. However, this turns out to be not the case as we plot the η-C_i for a given P_μ and different $\dot{m}$. This is demonstrated in Fig. 7 at 37W.

With this method as well, α is estimated to be in the 0.37 to 0.44 range for different values of P_μ.

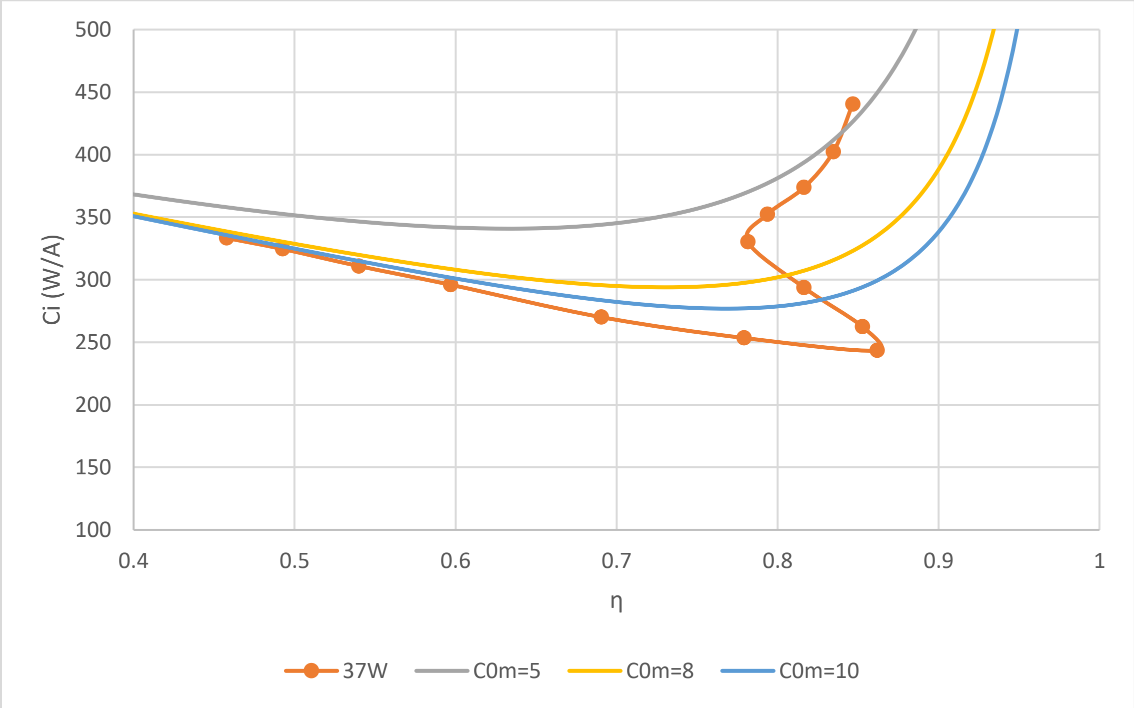

Figure 7. Demonstrating the Curve Fitting Approach at 37W Operation

B. Cathodoluminescent Probe Demonstration

Cathodoluminescence is the phenomenon observed in semiconductors exposed to an e^- beam producing visible light. Its intensity can be represented as[7]:

$$I_{CL} = f(J_e, E_e, material) \tag{7}$$

A low band gap semiconductor could hence be turned into a non-invasive plasma diagnostics tool, as inside plasma (with I^+ neutralizing the e^- charge) no bias is needed.

ZnO:Zn (produced by Nichia) was selected as luminescent material. In our design, this will be applied to the tip of an optical fiber core quartz rod, connected to an optical fiber cable. This would allow to directly measure α in the ECR region of μ10.

Through a series of experiments with the neutralizer utilized as an electron source, it was demonstrated how ZnO:Zn responds linearly to increasing current densities J_e, while it's not responsive to variations of electron energy E_e (approximation valid for energies lower than 20eV). As shown in Fig. 8, for pure electron exposure luminescence saturates at a certain J_e, while this doesn't occur for plasma exposure.

Experiments at high plasma density, however, pointed out how stable cathodoluminescence couldn't be achieved with ZnO:Zn. Hence, while the method is certainly applicable to different experiments, it turns out not to be a valuable tool to measure α.

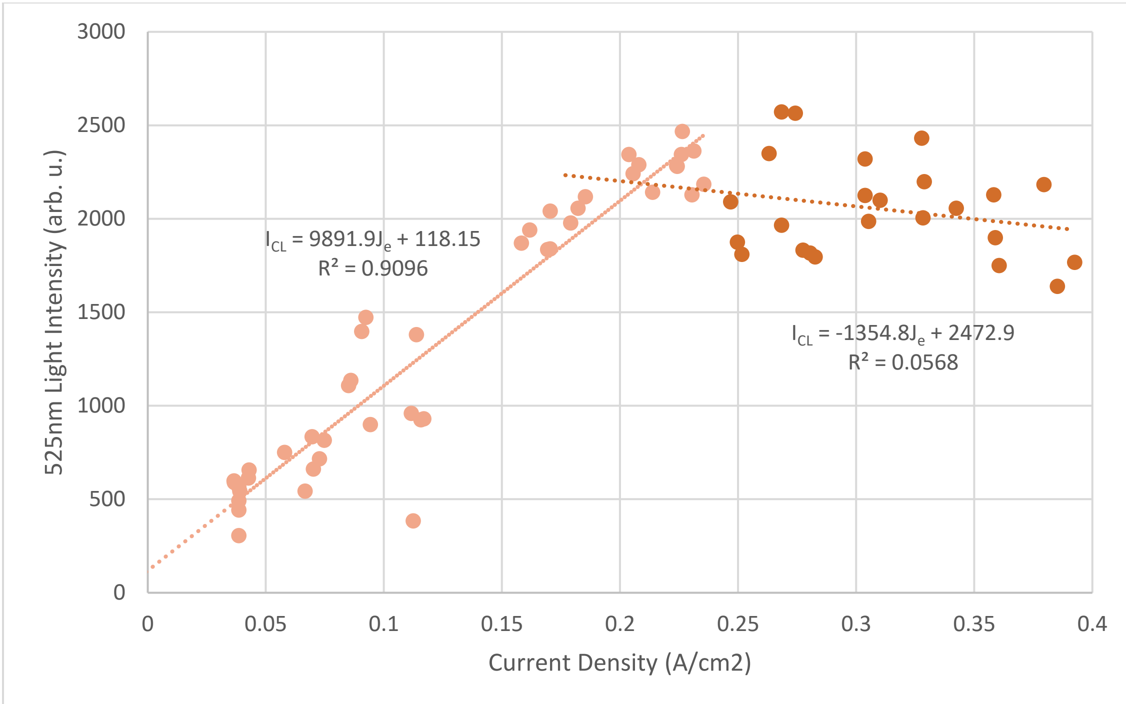

Figure 8. ZnO:Zn Cathodoluminescence at 525nm as Function of Je

V.Conclusions

The *Active-Passive-Loss* regions model has been developed and verified. Combined with the non-isothermal diffusion theory, it improved our understanding of the μ10 discharge chamber and is supporting the design of advanced magnetic circuits.

α was obtained with Langmuir probes, and it was pointed out how its value is affected by P_μ and not by $\dot{m}$. The values measured were confirmed by the curve fitting approach.

The feasibility of an optical probe based on ZnO:Zn cathodoluminescence for measuring currents in plasma was demonstrated, although the current design proved to be not applicable to our case.

References

[1]Brophy, J. R., & Wilbur, P. J. (1985). Simple performance model for ring and line cusp ion thrusters. AIAA journal, 23(11), 1731-1736.

[2]Chen, F. F. (2012). Introduction to plasma physics. Springer Science & Business Media.

[3]CORAL, G., TSUKIZAKI, R., NISHIYAMA, K., & KUNINAKA, H. (2016). ECR イオン源におけるマイクロ波電力吸収効率の計測. 宇宙科学技術連合講演会講演集, 60, 4p.

[4]Goebel, D. M., & Katz, I. (2008). Fundamentals of electric propulsion: ion and Hall thrusters (Vol. 1). John Wiley & Sons.

[5]Ise, T., Tsukizaki, R., Togo, H., Koizumi, H., & Kuninaka, H. (2012). Electric field measurement in microwave discharge ion thruster with electro-optic probe. Review of Scientific Instruments, 83(12), 124702.

[6]Kuninaka, H., & Satori, S. (1998). Development and demonstration of a cathodeless electron cyclotron resonance ion thruster. Journal of Propulsion and Power, 14(6), 1022-1026.

[7]Pennebaker, W. B., & Hanlon, J. O. (1974). Low-energy cathodoluminescence of ZnO: The ZnO-plasma display. Journal of Applied Physics, 45(3), 1315-1322.

[8] 谷義隆, 神田大樹, 月崎竜童, 細田聡史, 西山和孝, & 國中均. (2017). マイクロ波放電式イオンエンジンの性能向上に関する研究. In title 平成 28 年度宇宙輸送シンポジウム: 講演集録 FY2016.

[9]Tsukizaki, R., Koizumi, H., Hosoda, S., Nishiyama, K., & Kuninaka, H. (2010). Improvement of the Thrust Force of the ECR Ion Thruster μ10. TRANSACTIONS OF THE JAPAN SOCIETY FOR AERONAUTICAL AND SPACE SCIENCES, AEROSPACE TECHNOLOGY JAPAN, 8(ists27), Pb_67-Pb_72.

[10] 月崎竜童, 山本雄大, 細田聡史, 西山和孝, & 國中均. (2017). マイクロ波放電式イオンスラスタにおける 放電室分割による推進性能への影響. 日本航空宇宙学会論文集, 65(1), 17-20.

[11]Usui, M., Nishiyama, K., & Kuninaka, H. (2007). Analytical Model on Ion Production in Microwave Discharge Plasma Source. In 43rd AIAA/ASME/SAE/ASEE Joint Propulsion Conference & Exhibit (p. 5291).